Materials and Design 132 (2017) 496–504

Contents lists available at ScienceDirect

Materials and Design

journal homepage: www.elsevier.com/locate/matdes

Analysis of the shrinkage of injection-molded fiber-reinforced thin-wall parts

Davide Masato [a,*], Jitendra Rathore [a,b], Marco Sorgato [a], Simone Carmignato [b], Giovanni Lucchetta [a]

[a] Department of Industrial Engineering, University of Padua, Padua, (Italy)
[b] Department of Management and Engineering, University of Padua, Vicenza, (Italy)

HIGHLIGHTS

- Thin-wall injection molding of fiber-reinforced parts is characterized by a high shear-stressed melt flow.
- The shrinkage in the transverse direction is reduced by increasing the melt temperature and the injection speed.
- Injection molding processing affects fiber orientation: high values of melt temperature and injection speed reduces it.
- The extremely thin cavity yielded an almost flat trend of the orientation tensor indicating the absence of the core layer.
- Dimensional accuracy of thin-wall parts is optimized by high values of melt temperature, packing pressure, injection speed.

GRAPHICAL ABSTRACT

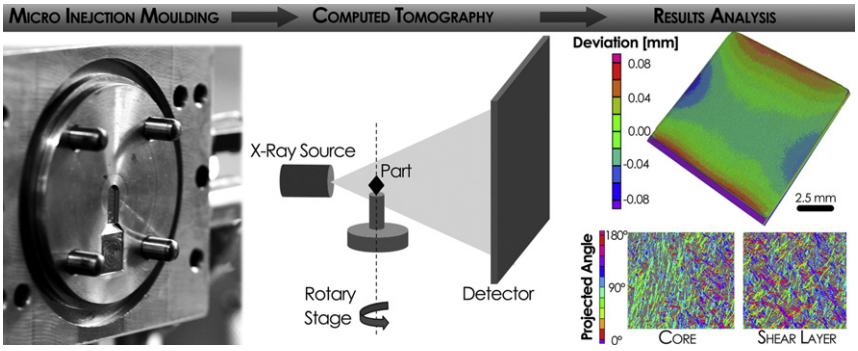

ARTICLE INFO

Article history:
Received 21 February 2017
Received in revised form 15 July 2017
Accepted 18 July 2017
Available online 18 July 2017

Keywords:
Thin-wall injection molding
Shrinkage
Fiber orientation
Computed tomography
Skin-shear-core morphology

ABSTRACT

Injection molding of thin-wall parts is characterized by a highly shear-stressed melt flow, which could affect the morphology of the moldings and consequently their shrinkage and warpage. This study focuses on the impact of injection molding processing conditions on dimensional accuracy of thin-wall fiber-reinforced parts. The reduction of shrinkage was taken in consideration by analyzing how the processing parameters affected the final dimensions of a 350 μm thick part. Moreover, the relation between the distribution of short glass fibers within the part and its dimensional accuracy was investigated by means of X-ray computed tomography. The experimental results showed that melt temperature and packing pressure were the processing parameters that most affected the shrinkage of thin-wall parts. In particular, a selection of high values for these parameters allowed for the minimization of the dimensional difference between the mold and the final parts. The analysis of the cross sections of the moldings allowed the observation of an almost flat trend of the orientation tensor for parts molded at lower injection speed, indicating the absence of the core layer. This caused a higher shrinkage along the cross-flow direction that eventually led to a differential shrinkage and to the warpage of the final part.

1. Introduction

Injection molding (IM) is nowadays one of the most flexible, reliable and cost effective manufacturing technologies to produce complex plastic components [1]. Precision manufacturing of parts produced by IM

* Corresponding author at: Department of Industrial Engineering, University of Padova, via Venezia 1, 35131 Padova, Italy.
E-mail address: davide.masato@phd.unipd.it (D. Masato).

http://dx.doi.org/10.1016/j.matdes.2017.07.032
0264-1275/

Nomenclature

IM	injection molding
μ-CT	X-ray micro computed tomography
T_b	melt temperature
V_{inj}	injection speed
P_h	packing pressure
S_f	shrinkage in the flow direction
S_t	shrinkage in the transverse direction
L_{fpart}, L_{tpart}	molded part dimensions in the flow and transverse directions
L_{fmold}, L_{tmold}	mold cavity dimensions in the flow and transverse directions

recently attracted large attention for electronics applications, including connectors, because of their increasing market trends [2]. Despite the trend of miniaturization observed for IM applications, connectors remain relatively large, because of their complex design, which poses several manufacturing issues [3]. In particular, the thin wall that characterizes their typical geometry constitutes a major manufacturing constraint [4]. Hence, the commercial breakthrough of new and smaller connectors strongly depends on the necessity to develop low cost mass production technologies, which can provide dimensional accuracy and good part quality [5].

It has been demonstrated in the literature that quality and dimensional accuracy of injection-molded parts characterized by small thickness mainly depends on the injected polymer [6], the part geometry, the mold design and the selection of process variables [7]. Shrinkage and warpage are common defects resulting from the IM process that can impair quality and functionality of final parts [8]. In this sense, reducing and controlling shrinkage is very important to control dimensional accuracy of products, especially when manufacturing parts characterized by tight tolerances [9].

The intrinsic cause for polymer shrinkage is the thermodynamic behavior of polymers, which is responsible for dimensional variations in injection-molded parts. In order to guarantee process quality, it is then important to minimize the difference between the mold and the part dimensions, especially for applications requiring tight fit tolerances.

When dealing with injection molding, it is necessary to control many process parameters that can influence the dimensional accuracy of the parts by altering their shrinkage behavior [10]. For this reason, it is important to understand the effect of the controllable process parameters in order to improve the quality of the final parts. In general, shrinkage minimization of injection-molded parts is better performed with the adoption of statistical approaches [11]. Researchers reported in the literature that the main injection molding parameters affecting the overall shrinkage are cooling time, packing pressure [12,13], melt temperature [14] and injection speed [15]. However, the identification of the most critical processing parameters influencing the dimensional accuracy cannot be separated from material properties and part design [16]. The combination of these factors in the case of thin-wall parts makes the shrinkage behavior and the process parameters selection particularly critical.

The achievement of structural and thermal stability are fundamental requirements for the manufacturing of micro connectors, thus leading to the selection of high performance materials, characterized by good mechanical and thermal properties, such as fiber-filled polymers [17]. However, the use of reinforced polymers poses some processing issues, related to the anisotropic distribution of fibers within the parts, which eventually affects the shrinkage of the parts [18]. Azaman et al. numerically investigated the injection molding of thin-wall parts (thickness 0.70 mm) indicating that the presence of 10% weight glass fibers affect the shrinkage of the parts [19]. Glass fibers affect the shrinkage of thin-wall injection molded parts by modifying their morphology. Cadena-Perez et al. showed that the addition of fiber fillers completely change the shrinkage behavior of the polymer parts [20]. In particular, they showed their significant effect in the melt flow direction and the null effect in the transverse one.

The fiber orientation in injection-molded parts is determined and affected by the geometry of the mold and by the molding parameters [21]. Several researchers have studied how the fiber orientation tensor is influenced by the injection molding parameters [22,23]. Nevertheless, the correlation between fiber distribution and parts shrinkage has not been investigated for thin-wall parts yet.

Experimental studies about the IM process demonstrated that shrinkage is affected by scale effects [24], especially due to the different morphology of the parts, which is caused by the high shear rates that characterize the thin-wall IM process [25,26]. In general, fiber orientation within injection-molded parts is explained considering the 'fountain-flow' model [27]: the shear effect is more marked in the skin layer and consequently is the orientation in the melt flow direction; conversely, in the core region, the melt flow is subjected to the minimum shear and the orientation is considerably lower. However, this behavior can be modified by the diverse thickness ratio between the skin and core layers in the case of very small thickness [28].

Characterization of the skin-core morphology and of fiber orientation by means of optical observations of cross sections of the moldings can be very complex for thin-wall parts. In this sense, micro computed tomography (μ-CT) is a powerful technique to analyze fiber orientation [29]. As a non-destructive testing (NDT) method, μ-CT analysis can also eliminate the distortions introduced by sample cutting and preparation [30].

In this work, the effects of fiber orientation and process parameters on the dimensional accuracy of injection-molded thin-wall parts were experimentally investigated. The design of experiments (DoE) approach was used to understand the effects of IM process parameters on parts' shrinkage. The results of this first dimensional analysis were then complimented using μ-CT to characterize short glass fiber orientation and its correlation with the IM process. The resulting skin-shear-core morphology among the thin-wall parts was then characterized using μ-CT data, allowing the understanding of its relationship with the part shrinkage.

Section 2 describes the mold design and the manufacturing system adopted for the IM tests, as well as the approach to the experimentations. Section 3 discusses the characterization of the molded thin-wall parts, describing the approaches used for shrinkage measurements and for evaluation of fiber orientation. Section 4 analyzes and comments

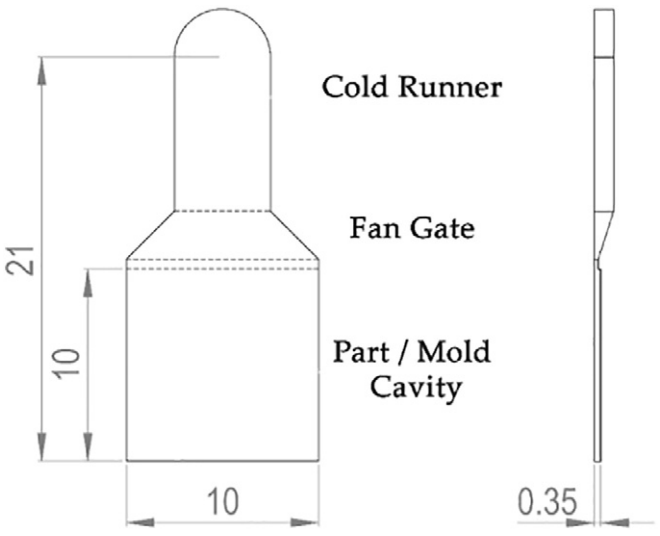

Fig. 1. Design of the study part. All dimensions are expressed in millimeters.

Table 1
Main properties of the Ultradur B4300 G2 PBT.

Property	Test method	Units	Value
Density	ISO 1183	g/cm^3	1.37
MVR (250 °C - 2.16 kg)	ISO 1133	cm^3/10 min	16
Melt temperature	ISO 11357	°C	250

Table 2
Process parameters settings for the shrinkage DoE plan.

Factor	Low level	High level
T_b (°C)	270	290
V_{inj} (mm/s)	200	600
P_h (bar)	200	600

the effects of the IM process on the dimensional variations of the parts and it reports the results of the fiber orientation analysis. Concluding, Section 5 summarizes the main findings of this work indicating how process parameters can be selected to improve the accuracy of thin-wall moldings.

2. Injection molding setup

2.1. Part and mold design

The part considered in this study is a square plaque with a side length of 10 mm, as shown in Fig. 1. The part was specifically designed to allow an accurate evaluation of the shrinkage and of the orientation tensor using μ-CT, according to conventional injection molding standards [31] and methodologies proposed in the literature for thin-wall parts [32]. In order to maximize the effect of the thin-wall mold cavity on the shrinkage, a thickness of 350 μm was chosen for the plaque.

In the mold, the square cavity was positioned on the moving half at the end of a fan gate (thickness: 0.2 mm), which ensured a linear flow front and a balanced filling. The polymer was fed through a fan gate and a runner with a rectangular cross-section (dimensions: 5 × 1 mm), directly connected to the nozzle of the IM machine.

The square cavity was machined with a 5-axis micro-milling machine (Kugler, Micromaster 5×) and its dimensions were measured using a multi-sensor coordinate measuring machine (Werth, Video-Check-IP 400). The average dimensions of the cavity were of 9.899 mm in the flow direction and of 9.906 mm in the perpendicular direction.

In order to prevent a possible deformation of the part during the demolding phase, due to its reduced thickness, a single ejector with a diameter of 2 mm was positioned adjacent to the runner.

2.2. Material and manufacturing system

A commercial polybutylene terephthalate PBT (BASF, Ultradur B4300 G2) reinforced with short glass fibers (10% in weight) was used for the injection molding experiments. The material was selected because of its strength, stiffness and impact resistance, which make it suitable for electronics applications, such as housings, plugs and connectors. However, PBT is a semi-crystalline thermoplastic polymer thus being characterized by marked shrinkage properties, making its processing critical in terms of dimensional accuracy. This is especially critical for application requiring coupling with other components and it is accentuated for thin-wall parts, such as connectors. The main properties of the injected polymer are summarized in Table 1.

A micro IM machine (Wittmann Battenfeld, MicroPower 15) with a maximum injection speed of 750 mm/s and a maximum clamping force of 150 kN was used for the experiments. A mold heating system was realized using four electrical cartridges, two for each mold half. Two thermocouples allowed the control of two temperature zones, one for each mold half.

2.3. Experimental approach

A three-factor full factorial plan was designed to characterize the effect of the IM process on both shrinkage and fiber orientation of the thin-wall parts. In order to optimize the number of experiments, the DoE was designed to have two levels of variations for the selected parameters. One of the important factors considered in the optimization was the long scanning time required in CT analysis. In particular, each repetition for each run of the DoE plan took around 4 h, which is due to the low power of the X-ray source and the high exposure time of the X-ray detector that were set for obtaining good quality CT data.

The parameters selected for the investigation were melt temperature T_b, injection speed V_{inj} and packing pressure P_h. The range values for the DoE plan (reported in Table 2) and the fixed parameters values were defined considering the literature, recommendations of the material supplier (e.g. max. nozzle melt temperature, mold temperature) and technological limitations of the available experimental setup. The upper and lower values of the DoE parameters were designed to cover a wide range of variation for each one of the selected process parameters. Furthermore, the process window was specifically designed to consider the complexity of the geometry and the characteristics of the molding polymer.

During the IM tests, the following parameters were fixed:

- mold temperature: 80 °C;
- metering size: 7.5 mm^3;

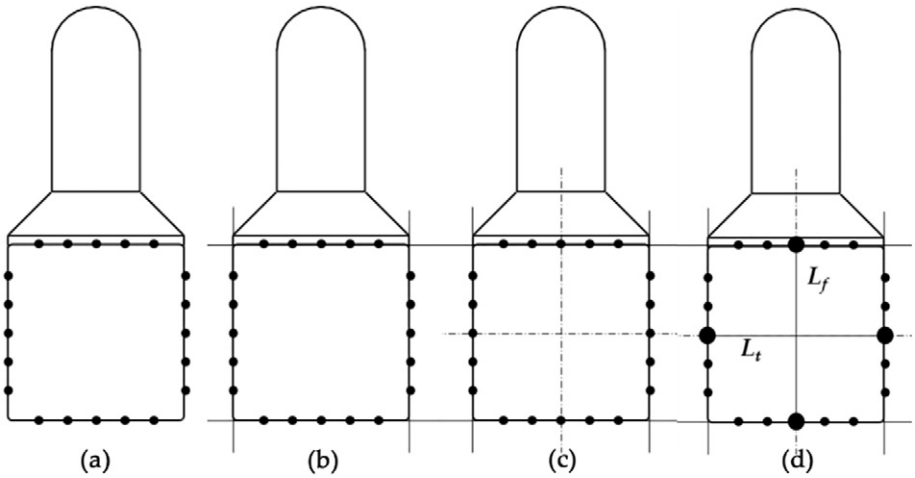

Fig. 2. Procedure adopted to evaluate the dimensions of molded thin-wall parts.

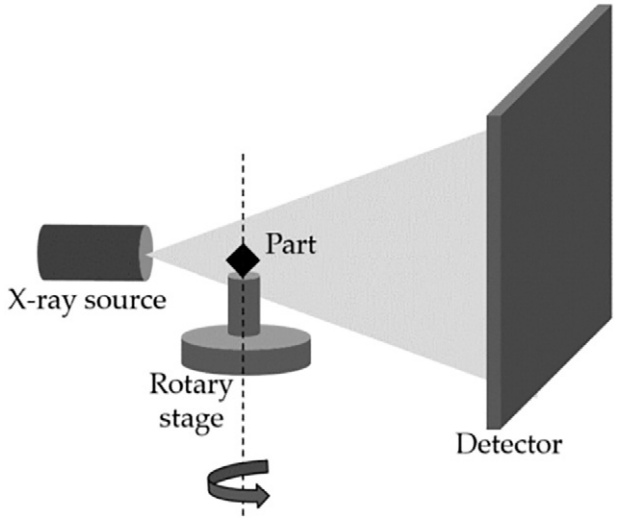

Fig. 3. Schematic representation of the μ-CT measuring system.

- velocity/pressure switch-over point: 90% of maximum injection pressure;
- packing time: 2 s;
- cooling time: 3 s;
- clamping force: 150 kN.

The response variables selected for the DoE campaign were the shrinkage (in the flow direction S_f and in the transverse direction S_t respectively) and the average and the maximum values of the orientation tensor (evaluated along the flow direction).

To guarantee the stability of the injection molding process, for each run of the DoE plan, ten molding cycles were carried out before the collection of the first part. Then, three parts were collected for the shrinkage and fiber orientation characterization, one every five molding cycles, for each combination of molding conditions. Summarizing, the experimental campaign comprised the molding of more than a hundred parts and the collection of 24 moldings for the characterization and the computation of all the selected response variables.

3. Characterization of the molded parts

3.1. Dimensional measurements

The linear shrinkage of the molded thin-wall parts was determined according to Fischer's definition as the "difference between the linear dimension of the mold at room temperature and that of the molded part at room temperature within 48 hours following the ejection" [33].

The dimensional measurements of the parts were evaluated by means of a multi-sensor coordinate measuring machine (Werth, Video-Check-IP 400), using a video imaging sensor and a direct episcopic illumination, which allowed identifying the edges of the samples [34]. The following measuring procedure was applied (Fig. 2):

Table 3
Parameters used for the μ-CT scans.

Parameter	Unit	Value
Voltage	kV	95
Current	μA	74
Exposure time	s	2.8
Number of projections	–	2500
Averaging	–	2
Physical filtering	–	No
Voxel size	μm	8.3
Scanning time	hours	3.9

Table 4
Results of the experimental campaign for each run of the factorial plan.

T_b (°C)	V_{inj} (mm/s)	P_h (bar)	S_f (%)		S_t (%)		Avg. orientation		Max. orientation	
			Avg. Val.	Std. Dev.	Avg. Val.	Std. Dev.	Avg. Val.	Std. Dev.	Avg. Val.	Std. Dev.
270	200	200	0.91	0.05	1.63	0.03	0.73	0.01	0.80	0.01
290	200	200	0.84	0.01	1.41	0.04	0.67	0.01	0.75	0.02
270	600	200	0.97	0.03	1.33	0.05	0.62	0.01	0.74	0.01
290	600	200	1.01	0.04	1.34	0.03	0.61	0.01	0.68	0.01
270	200	600	0.62	0.05	1.13	0.06	0.70	0.01	0.79	0.01
290	200	600	0.54	0.06	1.05	0.03	0.68	0.01	0.78	0.02
270	600	600	0.57	0.03	0.94	0.04	0.64	0.01	0.73	0.01
290	600	600	0.55	0.05	0.78	0.02	0.58	0.01	0.65	0.01

(i) acquisition of the coordinates of five equally spaced points for each edge of the square molded parts - Fig. 2 (a);
(ii) association of a straight line for each one of the plaque edges by fitting to the acquired points - Fig. 2 (b);
(iii) creation of two symmetry lines in the flow and transverse directions, followed by intersection of the symmetry lines with the lines representing the edges of the specimen, to determine a midpoint for each edge - Fig. 2 (c);
(iv) evaluation of the dimensions as the distance between the midpoints on the opposite edges of the parts - Fig. 2 (d).

3.2. Shrinkage calculation

The shrinkage of the molded parts was calculated as a percentage reduction from mold dimensions. The following equations were applied for each run of the DoE plan to obtain the response variables for the analysis:

$$S_f[\%] = \frac{L_{fpart} - L_{fmold}}{L_{fmold}} \cdot 100 \quad (1)$$

$$S_t[\%] = \frac{L_{tpart} - L_{tmold}}{L_{tmold}} \cdot 100 \quad (2)$$

where L_{fpart} and L_{tpart} are the dimensions of the molded part, measured with the coordinate measuring machine in the flow and transverse direction respectively; L_{fmold} and L_{tmold} are the dimensions of the mold in the two directions.

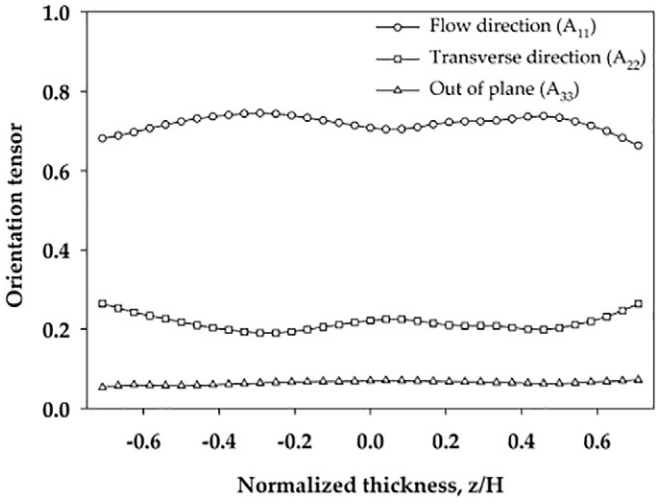

Fig. 4. Major components of the orientation tensor evaluated for the molded thin-wall parts using μ-CT.

Table 5
Results of the ANOVA considering shrinkage as the response variable.

Factor	*p*-Value	
	S_f	S_t
T_b	0.156	0.003
V_{inj}	0.056	0.000
P_h	0.000	0.000
$T_b \cdot V_{inj}$	0.048	0.274
$T_b \cdot P_h$	0.486	0.745
$V_{inj} \cdot P_h$	0.006	0.495

Table 6
Results of the ANOVA considering fiber orientation as the response variable.

Factor	*p*-Value	
	Avg. orientation	Max. orientation
T_b	0.000	0.000
V_{inj}	0.000	0.000
P_h	0.467	0.613
$T_b \cdot V_{inj}$	0.550	0.007
$T_b \cdot P_h$	0.559	0.366
$V_{inj} \cdot P_h$	0.873	0.051

3.3. Fiber orientation measurements

X-ray computed tomography (CT) is an emerging technology for dimensional quality control and non-destructive testing [35]. In comparison to other measuring techniques, CT offers the advantage of providing a non-destructive 3D measurement also of the internal structures, such as fibers.

A metrological μ-CT system (Nikon Metrology, X-Tek MCT 225) was used for measuring the molded parts and analyzing their fiber orientation. The metrological performances of the CT system were evaluated using specific procedures and a fiber-based calibrated object [36,37].

The X-ray projections were acquired for a complete rotation cycle (see Fig. 3) and subsequently reconstructed into a 3D volumetric dataset. The CT metrological software VGStudio MAX 3.0 (Volume Graphics GmbH, Germany) was used to process and evaluate the acquired data. Table 3 reports the parameters employed for the μ-CT scans.

The acquired datasets were analyzed by calculating the orientation tensor within a selected region of interest (dimensions: 5 × 5 mm) along the whole thickness of the molded thin-wall parts. The three-dimensional orientation was described using a second order tensor as suggested by Advani and Tucker [38]. The major components of the tensor are A_{11}, A_{22}, A_{33}, which represents the orientation in the flow direction, the transverse direction and the out of the plane direction. Fig. 4 reports the results of the fiber orientation analysis performed on the thin-wall molded samples in the three directions.

In injection molding, because of their kinematics, the fibers are mainly oriented in the flow direction and A_{11} is the highest component. For this reason, the molded parts in the following experiments were characterized considering the orientation in the melt flow direction, which contains the quantitative information about the microstructure and is the most sensitive to flow, processing and material changes.

4. Results and discussion

The results of the experimental campaign were analyzed collecting each one of the selected response variable (i.e. shrinkage in parallel and perpendicular direction, maximum and average values of the main component of the fiber orientation tensor). Table 4 shows the average values and the standard deviations for each run of the DoE experimental plan.

For each treatment, the factorial design was analyzed in order to evaluate the factors and the first-order interactions that significantly affect the selected response variables. A General Linear Model was used to perform a univariate analysis of variance (ANOVA) for the designed factorial plan. The terms included in the model are all the main factors implemented in the design of the experimental plan. The statistical identification of significant parameters was carried out considering the *p*-values, for which the threshold value was fixed at 0.05. Then, factors having a *p*-value inferior to 0.05 are statistically significant to the selected response.

The results of the ANOVA showed that among the selected processing parameters only the packing pressure (−8%) is affecting shrinkage in both the melt flow and the transverse directions. The average shrinkage in the transverse direction is also reduced by increasing the melt temperature (−9%) and the injection speed (−15%). Considering fiber orientation, the results indicate that a selection of higher values for both injection speed (−11%) and melt temperature (−7%) yield a reduction of fiber orientation. The results of the analysis of variance are further presented with more details and explanation in the next sections.

4.1. Effect of process parameters on shrinkage

The results of the analysis of variance (Table 5) indicated that all the considered IM parameters are significantly affecting the shrinkage of the thin-wall parts in the transverse direction (S_t). Conversely, considering the flow direction (S_f) the packing pressure is the only significant parameter.

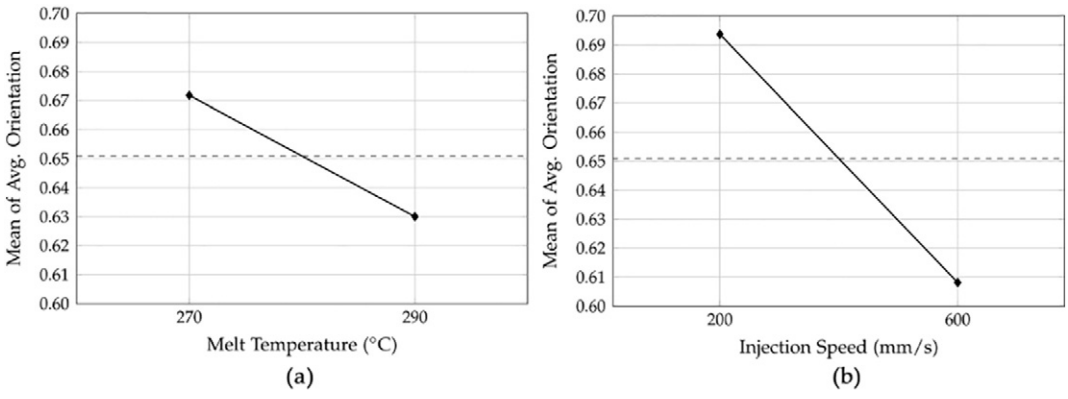

Fig. 5. Effect of (a) melt temperature and (b) injection speed on the average orientation of fibers.

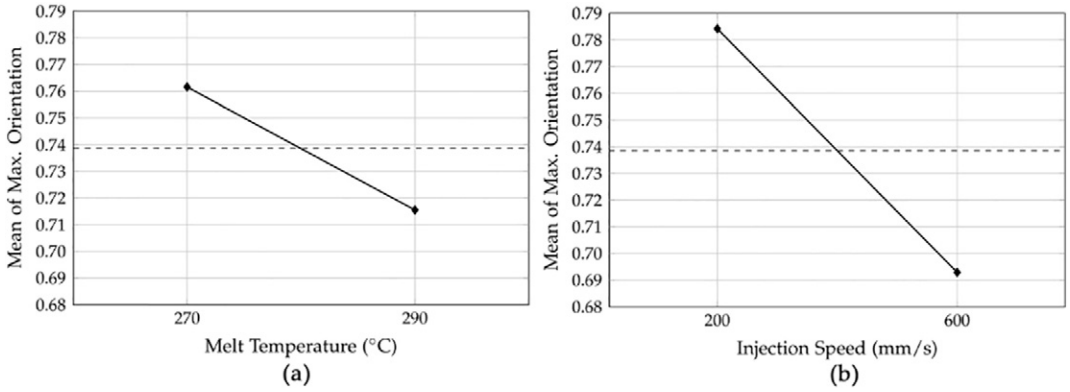

Fig. 6. Effect of (a) melt temperature and (b) injection speed on the maximum orientation of fibers.

By varying the packing pressure from 200 to 600 bar, the shrinkage reduces by 35% in the flow direction and by 31% in the transverse direction. Indeed, in agreement with the compressibility of the polymer, the higher the pressure applied to the polymer the lower its specific volume and its shrinkage.

The shrinkage of the thin-wall parts in the transverse direction was reduced by high values of both melt temperature and injection speed. In particular, the main effect of increasing the melt temperature by 20 °C was a reduction of the shrinkage by 9%, while increasing the injection speed from 200 to 600 mm/s resulted in a decrease of S_t by 15%. Indeed, these parameters modified the shrinkage behavior of the thin-wall parts by changing heat convection during the filling phase and fiber orientation.

4.2. Effect of process parameters on fiber orientation

The fiber orientation tensor, obtained from the CT data, was analyzed using the VGStudio MAX 3.0 software. The main components of the orientation tensor (i.e. in the flow direction) were determined along the thin-wall parts thickness and the average and maximum values were used to perform the ANOVA for the DoE plan (Table 6). The main effects of both melt temperature and injection speed resulted statistically significant. Conversely, the packing pressure did not affect fiber orientation, as it was determined during the filling phase. The main effects of the statistically significant parameters were plot in Fig. 5 and Fig. 6 [39].

The melt temperature variation from 270 to 290 °C reduced the average orientation by 6.2% (Fig. 5 (a)) and the maximum orientation by 6% (Fig. 6 (a)). Indeed, increasing this parameter causes a slower solidification near the cavity walls and thus resulting in thinner shear layers within the thin-wall parts. Consequently, at higher melt temperature the number of oriented fibers, which are prevalent in the shear layers, decreases with the layers thickness.

The main effect of increasing the injection speed from 200 to 600 mm/s was a reduction of the average orientation by 12.3% (Fig. 5 (b)) and a reduction of the maximum orientation by 11.6% (Fig. 6 (b)). Certainly, changing the flow rate led to different kinematics for the fibers injected into the thin-walled cavity, modifying the skin-core morphology along the thickness.

Furthermore, the first order interaction between the two factors (T_b·V_{inj}) also resulted significant for the selected response variables (Fig. 7). In particular, when molding with a low injection speed the effect of a higher melt temperature was the reduction of the average and maximum fiber orientation by 3.1% and 1.9%, respectively. The trend becomes more evident at higher injection speed. An increase of 20 °C in the melt temperature caused a reduction of both the response variables by 10%. This is explained considering that at high injection speed the increased heat, convected by the polymer melt, counteracts more significantly the skin solidification and, therefore, the thickening of those shear layers that host the oriented fibers.

4.3. Skin-shear-core morphology

The fountain-flow filling pattern that characterizes the IM process generates a 5-layer structure composed of two surface (skin), two sub-surface (shear) and one core layer in the edge section. The resulting higher shear stress near the cavity walls inducted a marked fiber

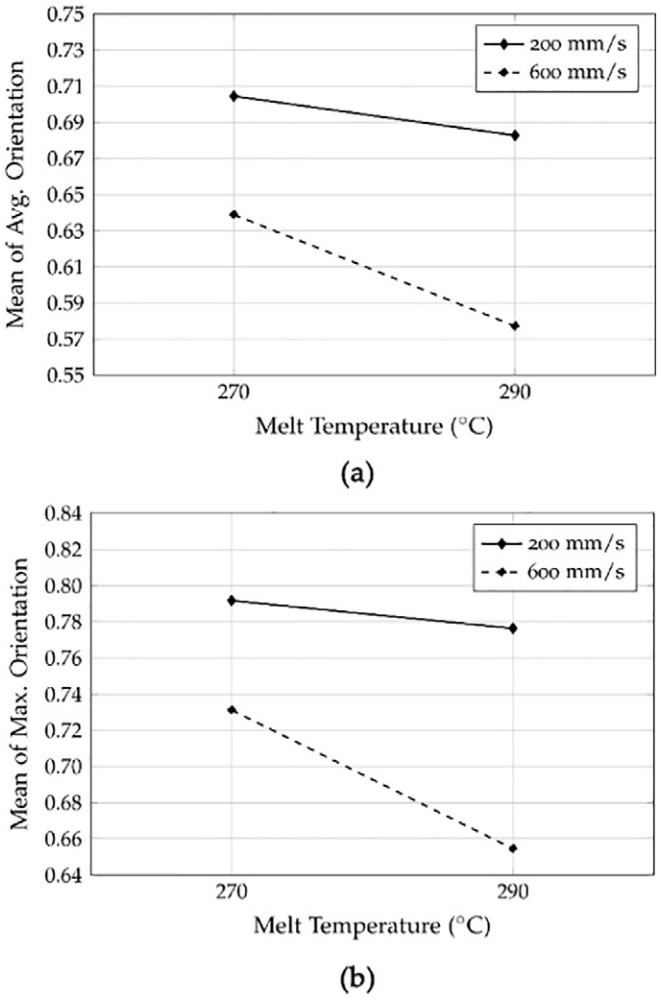

Fig. 7. Interaction plot between melt temperature and injection speed for (a) the average value and (b) the maximum value of the fiber orientation tensor.

orientation along the flow direction in the shear layers, and a more random distribution in the core (Fig. 8). However, the ratio between the shear and core layers, and the consequent overall fibers distribution, is affected by the IM process parameters, and in particular by the injection speed.

The higher fiber orientation observed at lower injection speed (Fig. 8 (a)) was explained considering the formation of thicker shear layers. In fact, the lower the flow rate, the higher the cooling rate between the polymer melt and the mold, hence allowing for a thinner core and consequently a higher overall orientation. Conversely, at higher injection speed the orientation in the shear layers is lower, as shown in Fig. 8 (b).

The analysis of the orientation tensor also indicated that the thickness ratio between the shear and core layers is very high compared to conventional injection molding due to the very small depth of the mold cavity. In conventional injection molding, the orientation of the fibers is markedly higher in the shear layers (i.e. in the proximity of the cavity walls) and orientation tensors indicate higher value of the orientation tensor components. Conversely, in thin-wall injection molding, the extremely reduced cavity thickness resulted in an almost flat pattern of the orientation tensor. However, the skin-shear-core morphology of the molded parts was modified by different selection of the injection molding process parameters. For parts molded at lower injection speed, especially for a high melt temperature (Fig. 9 (a)). The trend was less evident at lower melt temperature as the orientation tensor indicated higher orientation in the shear layers than in the core (Fig. 9 (b)), confirming the effect of the interaction between the investigated IM parameters (Fig. 7). This indicates that, apart from differences induced by the variations of IM process parameters, the core layer was very thin and in some cases not even present.

The consequence of a higher orientation along the melt flow direction, observed for lower injection speed, is that the shrinkage of the thin-wall parts is markedly higher along the cross-flow direction. In fact, owing to their higher stiffness and lower thermal expansion coefficient, the fibers hinder the polymer matrix from shrinking in the flow direction. Hence, the result is the differential shrinkage of the molded thin-wall parts.

5. Conclusions

The main objective of the present study was the analysis of the impact of the injection molding processing conditions on the dimensional accuracy of thin-wall fiber-reinforced parts. The shrinkage reduction, which is related to the pressure and temperature applied to the polymer during the process, was taken into consideration analyzing the final dimensions and the distribution of short glass fibers of a specifically designed thin-wall part.

The analysis of variance applied on the experimental data showed that among the selected processing parameters only the packing pressure (−8%) is affecting shrinkage in both the melt flow and the transverse directions. Moreover, shrinkage in the transverse direction was

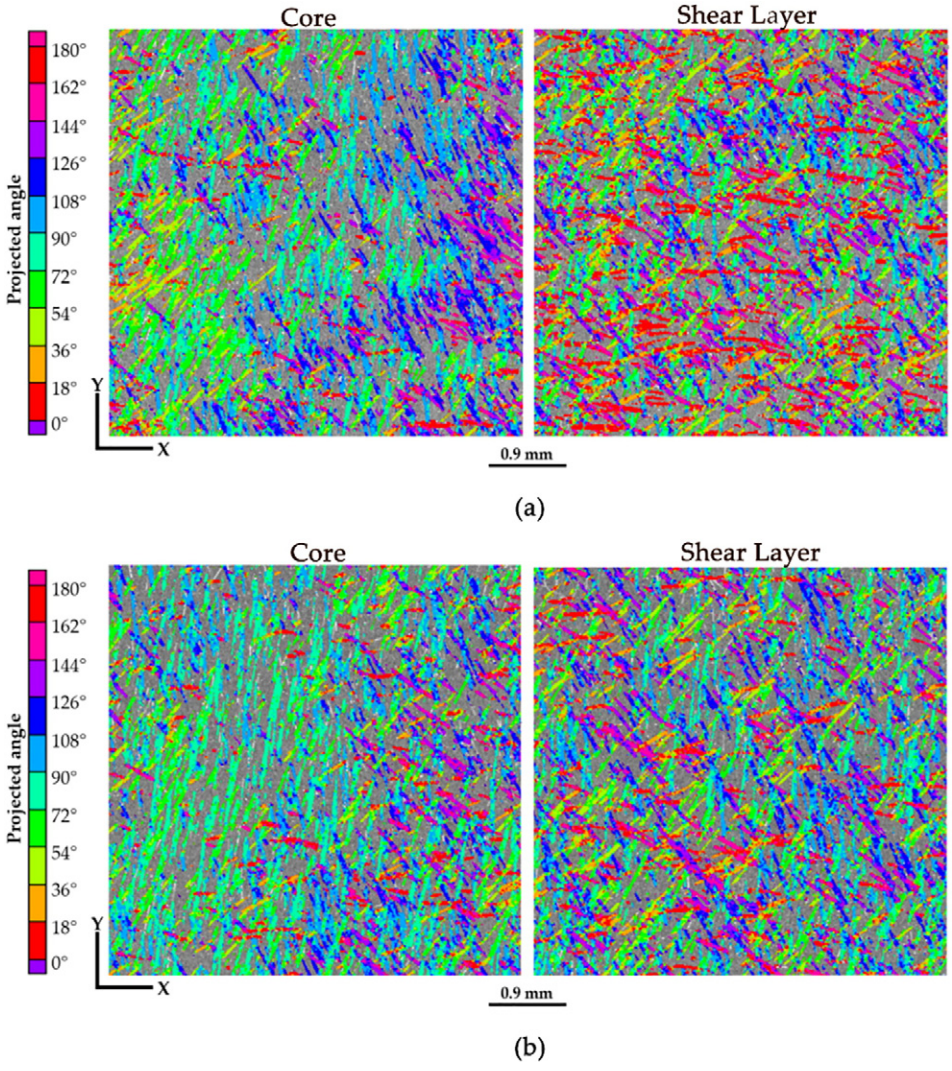

Fig. 8. Cross sections extracted form μ-CT 3D measurements of thin-wall parts molded at (a) low injection speed and (b) high injection speed.

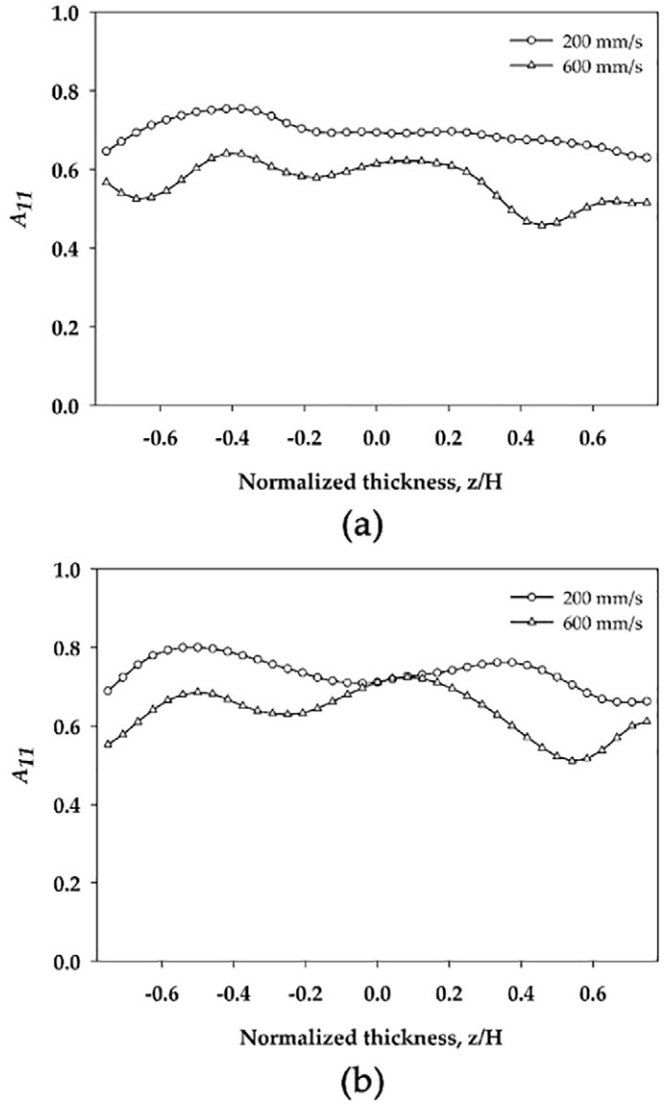

Fig. 9. Average fiber orientation tensors evaluated for parts molded at a melt temperature of (a) 290 °C and of (b) 270 °C.

further reduced by increasing the melt temperature (−9%) and the injection speed (−15%), due to their effect on fiber orientation along the thickness of the molded parts.

The analysis of fiber orientation within the thin-wall parts, performed using μ-CT, indicated that the injection molding process affected both average and maximum values of the orientation tensor. However, they were affected by different selection of process parameters. In particular, a selection of higher values for both injection speed (−11%) and melt temperature (−7%) yielded a reduction of fiber orientation.

The analysis of the cross sections of the thin-wall parts, obtained from μ-CT scans, allowed observing the 'skin-shear-core' morphology. The thickness ratio between the shear and core layers was affected by the process and in particular by the value of the flow rate. Indeed, the extremely thin cavity yielded an almost flat trend of the orientation tensor for parts molded at lower injection speed, indicating the absence of the core layer. The result was a higher shrinkage along the cross-flow direction that eventually led to a differential shrinkage and to the warpage of the final part.

In general, the results indicate how the dimensional accuracy of the molded thin-wall parts can be optimized by considering the effects of injection molding process parameters. In particular, the linear shrinkage of the molded parts was significantly reduced by adopting high values of the melt temperature, the packing pressure and the injection speed.

Further research will use the methodologies and the results of this analysis performed on a simple geometry part to extend process optimization on a real industrial application (e.g. a micro connector).

References

[1] C. Yang, X.H. Yin, G.M. Cheng, Microinjection molding of microsystem components: new aspects in improving performance, J. Micromech. Microeng. 23 (9) (2013), 093001.
[2] U. Wallrabe, H. Dittrich, G. Friedsam, T. Hanemann, J. Mohr, K. Müller, ... W. Zißler, Micromolded easy-assembly multi fiber connector: RibCon®, Microsyst. Technol. 8 (2–3) (2002) 83–87.
[3] G. Lucchetta, M. Sorgato, S. Carmignato, E. Savio, Investigating the technological limits of micro-injection molding in replicating high aspect ratio micro-structured surfaces, CIRP Annals-Manufacturing Technology 63 (1) (2014) 521–524.
[4] R. Selden, Thin wall molding of engineering plastics–a literature survey, Journal of Injection Molding Technology 4 (4) (2000) 159.
[5] H.J. Oh, D.J. Lee, C.G. Lee, K.Y. Jo, D.H. Lee, Y.S. Song, J.R. Youn, Warpage analysis of a micro-molded parts prepared with liquid crystalline polymer based composites, Compos. A: Appl. Sci. Manuf. 53 (2013) 34–45.
[6] M. Sorgato, D. Masato, G. Lucchetta, Effect of vacuum venting and mold wettability on the replication of micro-structured surfaces, Microsystem Technologies 2016, pp. 1–10.
[7] D. Masato, M. Sorgato, G. Lucchetta, Analysis of the influence of part thickness on the replication of micro-structured surfaces by injection molding, Mater. Des. 95 (2016) 219–224.
[8] S.J. Liao, D.Y. Chang, H.J. Chen, L.S. Tsou, J.R. Ho, H.T. Yau, ... Y.C. Su, Optimal process conditions of shrinkage and warpage of thin-wall parts, Polym. Eng. Sci. 44 (5) (2004) 917–928.
[9] D. Annicchiarico, J.R. Alcock, Review of factors that affect shrinkage of molded part in injection molding, Mater. Manuf. Process. 29 (6) (2014) 662–682.
[10] B. Ozcelik, I. Sonat, Warpage and structural analysis of thin shell plastic in the plastic injection molding, Mater. Des. 30 (2) (2009) 367–375.
[11] Y.C. Chiang, H.C. Cheng, C.F. Huang, J.L. Lee, Y. Lin, Y.K. Shen, Warpage phenomenon of thin-wall injection molding, Int. J. Adv. Manuf. Technol. 55 (5–8) (2011) 517–526.
[12] F. De Santis, R. Pantani, V. Speranza, G. Titomanlio, Analysis of shrinkage development of a semicrystalline polymer during injection molding, Ind. Eng. Chem. Res. 49 (5) (2010) 2469–2476.
[13] A.J. Pontes, A.S. Pouzada, Predicting shrinkage in semi-crystalline injection mouldings–the influence of pressure, Materials science forum, Vol. 514, Trans Tech Publications 2006, pp. 1501–1505.
[14] M. Altan, Reducing shrinkage in injection moldings via the Taguchi, ANOVA and neural network methods, Mater. Des. 31 (1) (2010) 599–604.
[15] J. Pomerleau, B. Sanschagrin, Injection molding shrinkage of PP: experimental progress, Polym. Eng. Sci. 46 (9) (2006) 1275–1283.
[16] A. Cellere, G. Lucchetta, Identification of CRIMS model parameters for warpage prediction in injection moulding simulation, Int. J. Mater. Form. 3 (1) (2010) 37–40.
[17] S.K. De, White, J. R. (Eds.)., Short Fibre-Polymer Composites, Elsevier, 1996.
[18] H. Sadabadi, M. Ghasemi, Effects of some injection molding process parameters on fiber orientation tensor of short glass fiber polystyrene composites (SGF/PS), J. Reinf. Plast. Compos. 26 (17) (2007) 1729–1741.
[19] M.D. Azaman, S.M. Sapuan, S. Sulaiman, E.S. Zainudin, A. Khalina, Numerical simulation analysis of unfilled and filled reinforced polypropylene on thin-walled parts formed using the injection-moulding process, International Journal of Polymer Science (2015), 659321.
[20] A.M. Cadena-Perez, I. Yañez-Flores, S. Sanchez-Valdes, O.S. Rodriguez-Fernandez, S. Fernandez-Tavizon, L.F.R. de Valle, J.L. Sanchez-Cuevas, Shrinkage reduction and morphological characterization of PP reinforced with glass fiber and nanoclay using functionalized PP as compatibilizer, Int. J. Mater. Form. 10 (2017) 233–240.
[21] H.M. Laun, Orientation effects and rheology of short glass fiber-reinforced thermoplastics, Colloid Polym. Sci. 262 (4) (1984) 257–269.
[22] P.F. Bright, R.J. Crowson, M.J. Folkes, A study of the effect of injection speed on fibre orientation in simple mouldings of short glass fibre-filled polypropylene, J. Mater. Sci. 13 (11) (1978) 2497–2506.
[23] P. Shokri, N. Bhatnagar, Effect of packing pressure on fiber orientation in injection molding of fiber-reinforced thermoplastics, Polym. Compos. 28 (2) (2007) 214–223.
[24] M.C. Huang, C.C. Tai, The effective factors in the warpage problem of an injection-molded part with a thin shell feature, J. Mater. Process. Technol. 110 (1) (2001) 1–9.
[25] J. Giboz, T. Copponnex, P. Mélé, Microinjection molding of thermoplastic polymers: morphological comparison with conventional injection molding, J. Micromech. Microeng. 19 (2) (2009), 025023.
[26] G. Lucchetta, D. Masato, M. Sorgato, L. Crema, E. Savio, Effects of different mould coatings on polymer filling flow in thin-wall injection moulding, CIRP Annals-Manufacturing Technology 1 (65) (2016) 537–540.
[27] W. Rose, Fluid-fluid interfaces in steady motion, Nature 191 (1961) 242–243.
[28] M. Vincent, T. Giroud, A. Clarke, C. Eberhardt, Description and modeling of fiber orientation in injection molding of fiber reinforced thermoplastics, Polymer 46 (17) (2005) 6719–6725.
[29] O. Wirjadi, M. Godehardt, K. Schladitz, B. Wagner, A. Rack, M. Gurka, ... A. Noll, Characterization of multilayer structures in fiber reinforced polymer employing synchrotron and laboratory X-ray CT, Int. J. Mater. Res. 105 (7) (2014) 645–654.
[30] H. Shen, S. Nutt, D. Hull, Direct observation and measurement of fiber architecture in short fiber-polymer composite foam through micro-CT imaging, Compos. Sci. Technol. 64 (13) (2004) 2113–2120.

[31] BS EN ISO 294-3, Plastics – Injection Moulding of Test Specimens of Thermoplastic Materials - Part 3: Small Plates, 2003.
[32] D. Annicchiarico, U.M. Attia, J.R. Alcock, A methodology for shrinkage measurement in micro-injection moulding, Polym. Test. 32 (4) (2013) 769–777.
[33] J. Fischer, Handbook of Molded Part Shrinkage and Warpage, 2012 (William Andrew).
[34] S. Carmignato, A. Voltan, E. Savio, Metrological performance of optical coordinate measuring machines under industrial conditions, CIRP Annals-Manufacturing Technology 59 (1) (2010) 497–500.
[35] L. De Chiffre, S. Carmignato, J.P. Kruth, R. Schmitt, A. Weckenmann, Industrial applications of computed tomography, CIRP Annals-Manufacturing Technology 63 (2) (2014) 655–677.
[36] S. Carmignato, D. Dreossi, L. Mancini, F. Marinello, G. Tromba, E. Savio, Testing of X-ray microtomography systems using a traceable geometrical standard, Meas. Sci. Technol. 20 (8) (2009), 084021.
[37] F. Marinello, E. Savio, S. Carmignato, L. De Chiffre, Calibration artefact for the micro-scale with high aspect ratio: the fiber gauge, CIRP Annals-Manufacturing Technology 57 (1) (2008) 497–500.
[38] S.G. Advani, C.L. Tucker III, The use of tensors to describe and predict fiber orientation in short fiber composites, J. Rheol. 31 (8) (1987) 751–784.
[39] D.C. Montgomery, Design and Analysis of Experiments, Vol. 7, Wiley, New York, 1984.